Electronic Supplementary Material (ESI) for Nanoscale.

Supporting Information

Tuning Coiled Coil Stability with Histidine-Metal Coordination

Isabell Tunn,[a] Alberto S. de Léon,[a] Kerstin G. Blank,[a]* Matthew J. Harrington[a,b]*

[a] I. Tunn, Dr. A. S. de Léon, Dr. K.G. Blank, Dr. M.J. Harrington
Max Planck Institute of Colloids and Interfaces, Science Park Potsdam-Golm, 14424 Potsdam, Germany, *E-mail: Kerstin.Blank@mpikg.mpg.de
[b] Dr. M.J. Harrington, McGill University, 801 Sherbrooke St. West, Montreal, Quebec H3A 0B8, Canada, *E-mail: Matt.Harrington@mcgill.ca

Table of Contents

1 Raman spectroscopy

All coiled coil (CC) peptides were obtained from a commercial supplier (Centic Biotech). They were synthesized using standard solid phase peptide synthesis methods and purified via HPLC (purity >95 %). Raman micro-spectroscopy was performed to study the CC secondary structure and His-Ni^{2+} coordination. The peptides HA_4 and HB_4 (no cysteine) were dissolved in ultrapure water to a concentration of approx. 5 mg ml^{-1}. The peptides were mixed in a 1:1 molar ratio to yield 0.5 mM HA_4HB_4. For investigating metal coordination, $NiCl_2$ was added to obtain a final concentration of 1 mM and the pH was raised to 8 using NaOH. HCl was added to obtain an acidic pH of ~4. The solution (5 µl) was dried on a coverslip. For the measurements of the resulting peptide films, a confocal Raman microscope (alpha300, WITec) was used. The microscope was equipped with a piezo scanner (P-500, Physik Instrumente) and a 50x objective (Nikon, NA 0.6). A linearly polarized laser (λ = 532 nm, Oxxius) was focused onto the sample with a polarization angle of 0° and no analyzer in the light path. The Raman scattered light was detected on a thermoelectrically cooled CCD detector (DU401A-BV, Andor) with an integration time of 2 s and 30 accumulations. Spectra from five different positions on the sample were collected and averaged. The measurement and subsequent data analysis were performed with the software ScanCtrlSpectroscopyPlus (Version 1.38, WITec) and Project FOUR (Version 4.1 WITec). OPUS was used for baseline correction (rubberband method, linear, 1 pt), and the spectra were normalized to the amide I peak at 1654 cm^{-1}.

2 CD spectroscopy

CD spectra were recorded to investigate the secondary structure and the thermal stability of the individual peptides as well as the CC in the absence and presence of $NiCl_2$. Peptide stock solutions were prepared in ultrapure water and their molar concentration was determined with amino acid analysis. The stock solutions were mixed in a 1:1 molar ratio and subsequently diluted in 10 mM PIPPS, 137 mM NaCl, 2.7 mM KCl, pH 8.1 (PIPPS BS) to obtain a final peptide concentration of 50 µM. For measurements in the presence of Ni^{2+}, $NiCl_2$ was added to the HA_4HB_4 solution (1:3 His:Ni^{2+}) before dilution with PIPPS BS. The CD spectra were acquired with a Chirascan qCD spectrometer (Applied Photophysics), equipped with a Peltier temperature controller (Quantum Northwest). A quartz cuvette (Hellma) with a path

length of 1 mm was used. All spectra were recorded from 200 nm to 250 nm with a step resolution of 1 nm and a bandwidth of 1 nm. The integration time (time per point) was set to 1 s nm^{-1}. The spectra were recorded at a temperature of 20 °C (three repeats). For baseline correction, the buffer spectra were recorded, using identical parameters, and subtracted from the peptide and CC spectra. The molar ellipticity $[\theta]$ [deg cm^2 $dmol^{-1}$] was calculated according to **Equation 1**:

$$[\theta] = \frac{100 \cdot \theta}{c \cdot d} \qquad (Equation\ 1)$$

with the ellipticity θ [deg], the concentration c [M] and the path length d [cm].[1]

Thermal unfolding of the samples was performed with temperature ramps from 4 to 90 °C, with a heating rate of 1 °C min^{-1}. Full spectra were recorded in 1 °C steps, using the same parameters as used for the single spectra with a shortened integration time of 0.7 s nm^{-1}. All measurements were performed in triplicate, unless stated otherwise. The melting temperature was determined from a global fit to all spectra in the range from 205 nm to 250 nm, using Global3 software (v. 1.6.0.0, Applied Photophysics). For fitting, a single transition was assumed and pre- and post-transition baseline correction was applied.

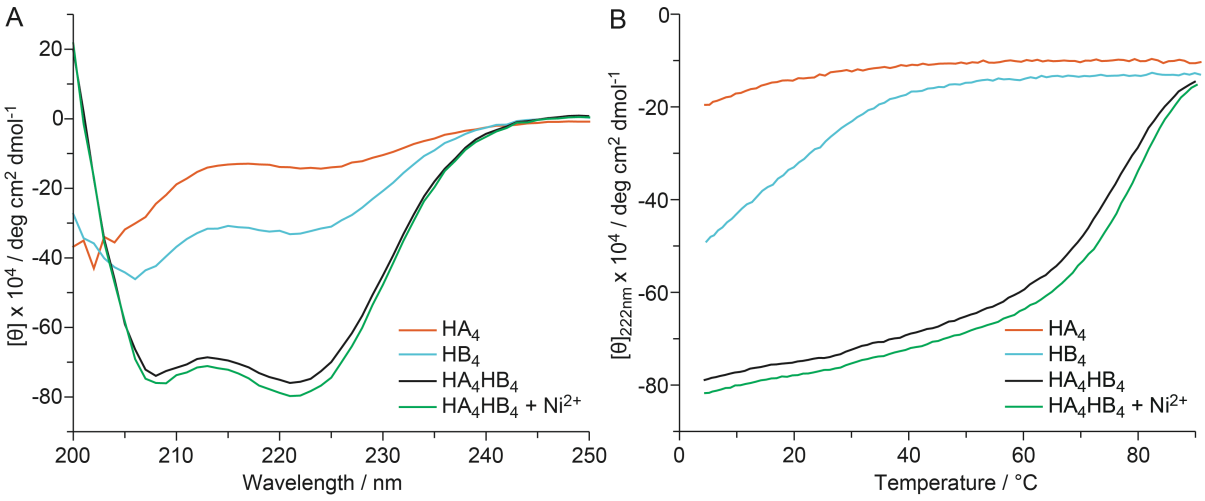

Fig. S1. CD spectra and thermal unfolding of the His-modified CC and the individual peptides. A) Full spectra at 20 °C. B) Thermal unfolding of the peptides. For visualization, the values at the minimum at 222 nm were extracted from all spectra measured. The total peptide concentration was 50 µM in 10 mM PIPPS BS, pH 8.1. The data for HA_4HB_4 are the average of three measurements. The individual peptides were measured only once.

Fig. S1A shows the full CD spectra of the individual peptides and of CC HA_4HB_4 with and without Ni^{2+}. The CD spectrum of the CC shows two characteristic minima at 208 nm and

222 nm, indicating α-helical secondary structure.[2] The ratio between the minima $r_{222/208}$ is 1.02, showing that HA_4 and HB_4 are forming a stable CC.[3] When Ni^{2+} is added (1:3 His:Ni^{2+}), the spectrum suggests a higher CC stability, evidenced by an increase of $r_{222/208}$ to 1.05 and a decrease of the absolute molar ellipticity. The individual peptides are largely unfolded. Thermal denaturation revealed that the individual peptides have a melting temperature T_m smaller than 4 °C (**Fig. S1B**). HA_4HB_4 shows a thermal stability of T_m = 76.4 ± 0.9 °C, which increases to 80.2 ± 0.6 °C in the presence of Ni^{2+}. The values represent the mean ± the standard error of the mean (SEM), n = 3.

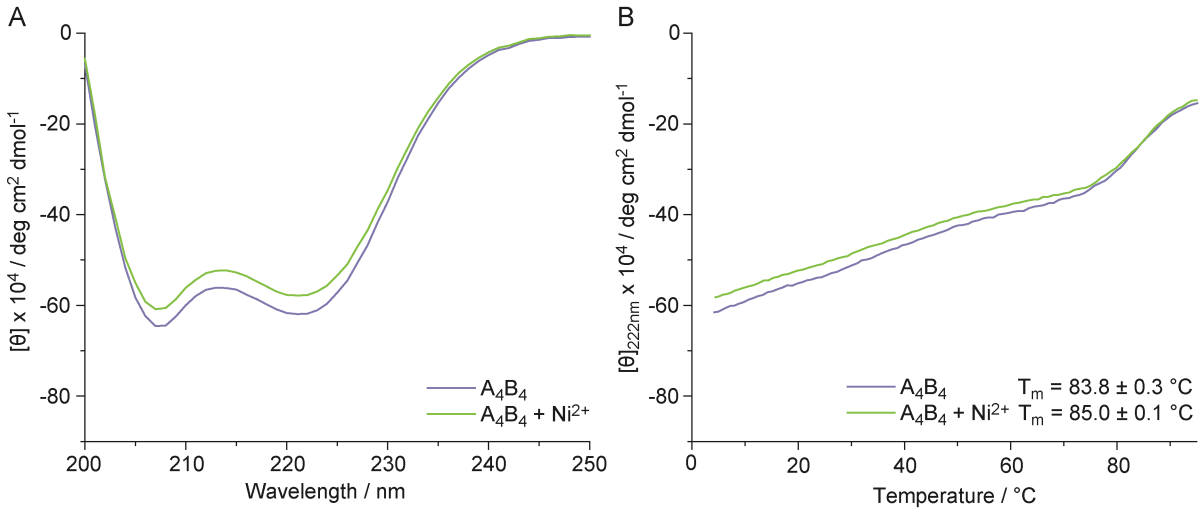

Fig. S2. CD spectra and thermal unfolding of the reference CC A_4B_4 without His. A) Full spectra at 20 °C. B) Thermal unfolding of the CC. For visualization, the values at the minimum at 222 nm were extracted from all spectra measured. The total peptide concentration was 50 µM in 10 mM PIPPS BS, pH 8.1. The data represent the mean ± SEM of three measurements.

CD spectroscopy was also performed with the reference CC A_4B_4 to demonstrate that the presence of Ni^{2+} alone has no influence on the conformation and stability of the CC (**Fig. S2**). A_4B_4 shows the characteristic minima for α-helical secondary structure. The thermal stability of A_4B_4 is identical in the absence (T_m = 83.8 ± 0.3 °C) and presence of Ni^{2+} (T_m = 85.0 ± 0.1 °C).

3 AFM-based single-molecule force spectroscopy (SMFS)

Surface and cantilever preparation for SMFS were performed as described in Zimmermann et al.[4] The cantilevers (MLCT, Bruker) were cleaned in an UV-ozone cleaner (BioForce Nanoscience) for 20 min. For amino-silanization, the cantilevers were submerged in pure 3-aminopropyl dimethyl ethoxysilane (APDMES) (ABCR) for 10 min at room temperature (RT)

and washed with isopropanol and ultrapure water. The cantilevers were cured for 30 min at 80 °C. The coverslips (Menzel Gläser) were sonicated for 10 min in isopropanol and 3x 5 min in water, followed by UV-ozone cleaning for 15 min. Amino-silanization was carried out in a solution of 1 % (v/v) ADPMES in absolute ethanol for 1 h. After washing 3x with isopropanol and water, the coverslips were cured at 80 °C for 1 h. Both surfaces were treated in parallel for the next steps. First, the NHS-ester of the heterobifunctional NHS-PEG-maleimide (10 kDa, Rapp Polymere) was coupled to the amino-functionalized surface. The PEG was dissolved to 30 mM in borate buffer (50 mM $H_3BO_3/Na_2B_4O_7$, pH 8.5) and incubated on the surfaces for 1 h in a humidity chamber at RT. The surfaces were washed intensively with water and dried under nitrogen flow. The peptides HA_4 and HB_4, carrying a cysteine at the desired terminus, were dissolved to 1.5 mM in coupling buffer (50 mM Na_2HPO_4, 50 mM NaCl, 10 mM EDTA, pH 7.2) and stored at -20 °C. Peptide stock solutions were diluted to 0.5 mM in coupling buffer. Peptide HB_4 was incubated on the cantilever and peptide HA_4 was incubated on the coverslip for 1 h in a humidity chamber at 4 °C. Finally, the surfaces were washed intensively with PIPPS BS to remove non-covalently bound peptides.

The SMFS measurements were performed with a ForceRobot 300 (JPK Instruments) at RT in PIPPS BS. Cantilever C with a nominal spring constant of 0.01 N m^{-1} was used. The spring constant was calibrated using the thermal noise method[5] after finalizing the measurement. The values ranged from 0.014 to 0.025 N m^{-1}. The relative set-point force was ~0.08 nN and the retract speed was varied (50, 200, 400, 1000, 2500, 5000 nm s^{-1}; 4000 nm s^{-1} for one data set with Ni^{2+}). Measurements were performed on a 10x10 µm grid with 8x8 points. To investigate the effect of Ni^{2+} coordination on CC stability, 1 mM $NiCl_2$ was added in the buffer.

The data were analyzed using the JPKSPM data processing software (Version 5.0.68, JPK Instruments). The force curves show the characteristic force extension behavior of the PEG linkers used to immobilize the CC. Note that the total length of two 10 kDa PEG linkers (one on the surface and one on the cantilever) is approx. 130 nm,[6] whereas the length of the folded CC is only 4 nm. The PEG linkers are used as an internal control, since their force extension behaviour can be fitted with the wormlike-chain (WLC) model[7] (**Equation 2**) in order to obtain the persistence length and the contour length:[8-9]

$$F(x) = \frac{k_B T}{l_p}\left(\frac{1}{4\left[1-\frac{x}{l_c}\right]^2} - \frac{1}{4} + \frac{x}{l_c}\right) \quad (Equation\ 2)$$

were F is the force, l_p the persistence length, l_c the contour length, x the end-to-end distance of the polymer chain, k_B the Boltzmann constant and T the temperature.

Only force curves that displayed a single rupture event (visual inspection), were fitted well with the WLC model and possessed a contour length larger than 90 nm (taking into account the polydispersity of the PEG) were considered for further analysis. These criteria efficiently eliminate force distance curves displaying non-specific binding events, which frequently possess much shorter contour lengths or cannot be fitted with the WLC model.

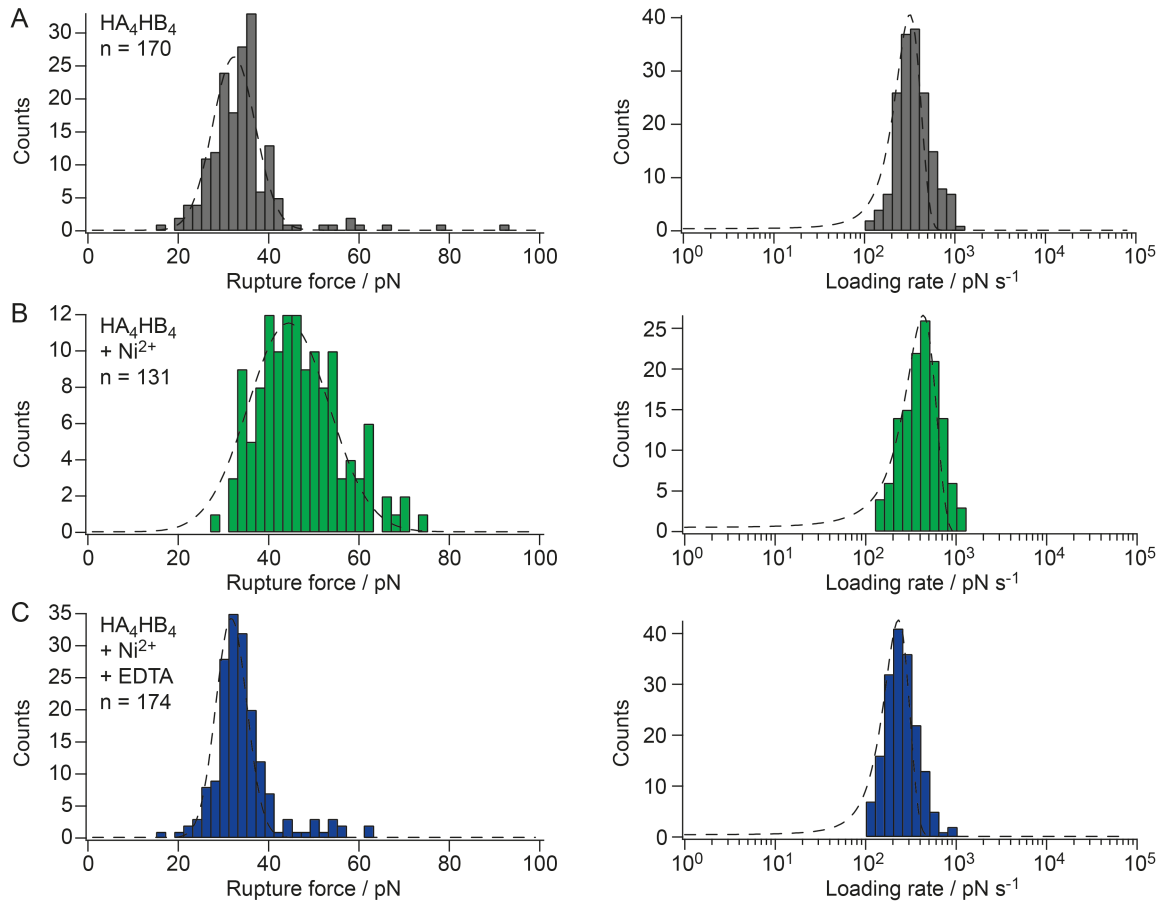

Fig. S3. Rupture force and loading rate histograms of HA_4HB_4 for a retract speed of 400 nm s^{-1}. A) Measurement without Ni^{2+}. The most probable rupture force F_R is 32.3 pN and the most probable $\dot{F}$ is 317 pN s^{-1}. B) Measurement with 1 mM Ni^{2+}. The most probable F_R is 44.4 pN at a loading rate $\dot{F}$ of 431 pN s^{-1}. C) Measurement with Ni^{2+} after washing with 10 mM EDTA. The most probable F_R is 31.7 pN at a loading rate $\dot{F}$ of 230 pN s^{-1}. The most probable values of F_R and $\dot{F}$ were obtained from a Gaussian fit to the histograms (dashed line); n represents the number of force curves included in each histogram.

The rupture forces (F_R) and the loading rates ($\dot{F} = dF/dt$) obtained from the JKPSPM data processing software were plotted into histograms. For each retract speed, the most probable rupture force and the most probable loading rate were determined using a

Gaussian fit to the corresponding histogram (logarithmic plot for $\dot{F}$) in IGOR Pro 6.37. Representative rupture force distributions obtained in the presence and absence of 1 mM Ni^{2+} and after washing with 10 mM EDTA are shown in **Fig. S3** (retract speed of 400 nm s^{-1}). The histograms show that the rupture force increased by ~10 pN in the presence of Ni^{2+}. This stabilization is reversed after washing the cantilever and surface with 10 mM EDTA. It should be noted that the histogram measured in the presence of Ni^{2+} is wider than the corresponding histograms in the absence of Ni^{2+} or after adding EDTA. We attribute this to the presence of multiple species, including CCs where zero, one or two helices contain an intact metal coordination bridge. **Fig. S4** and **S5** show one representative data set obtained from dynamic SMFS measurements performed in the absence and presence of 1 mM Ni^{2+}. A summary of the results from three independent measurements performed with different cantilevers and surfaces is given in **Tab. S1**.

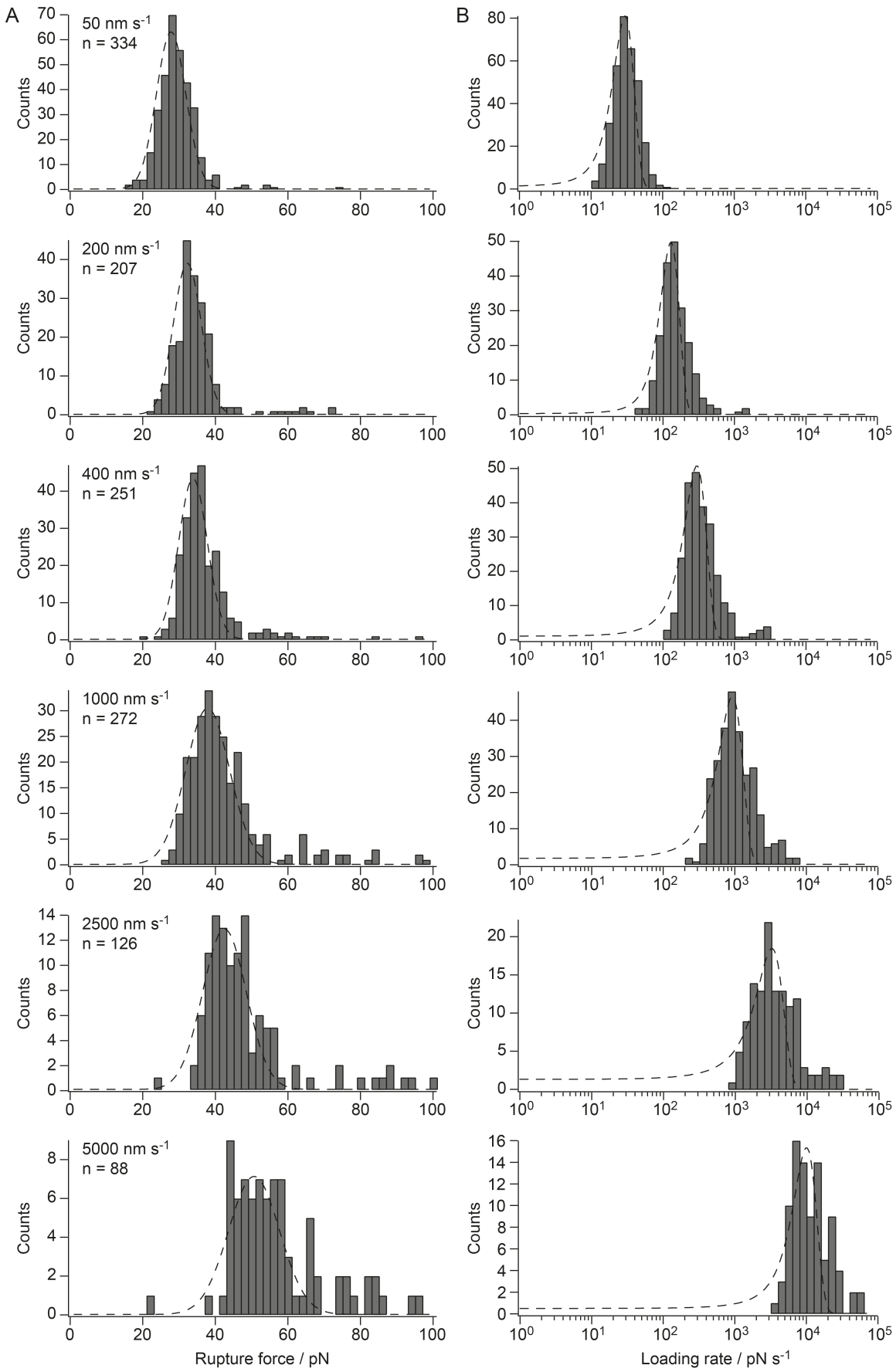

Fig. S4. Representative data set of a dynamic SMFS measurement of HA_4HB_4, performed in the absence of $NiCl_2$. A) Rupture force histograms obtained at the indicated retract speeds. B) Corresponding loading rate histograms (plotted logarithmically). The dashed line represents a Gaussian fit to the histograms to obtain the most probable rupture force and loading rate; n represents the number of force curves included in each histogram.

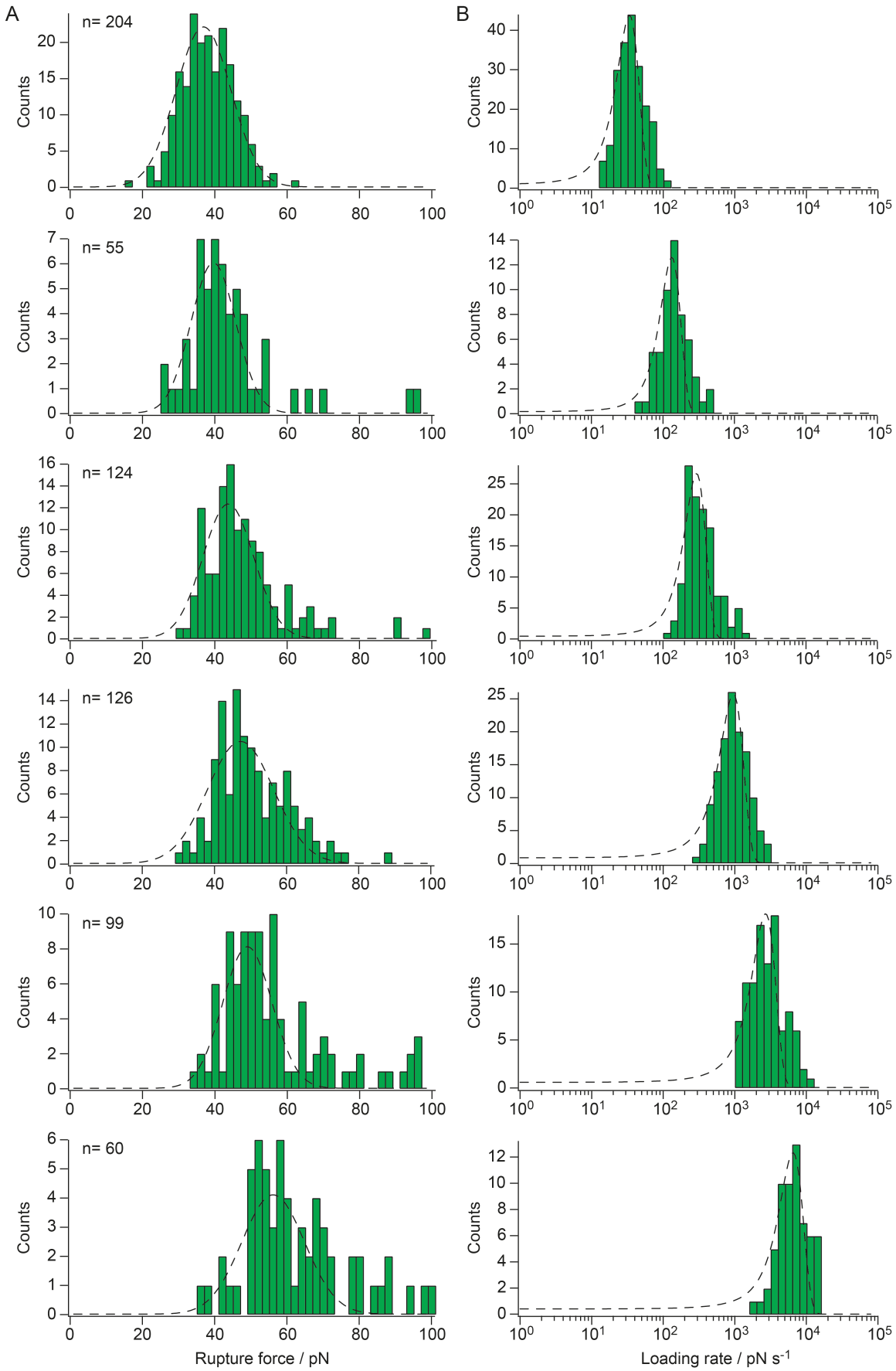

Fig. S5. Representative data set of a dynamic SMFS measurement of HA_4HB_4, performed in the presence of 1 mM $NiCl_2$. A) Rupture force histograms obtained at the indicated retract speeds. B) Corresponding loading rate histograms (plotted logarithmically). The dashed line represents a Gaussian fit to the histograms to obtain the most probable rupture force and loading rate; n represents the number of force curves included in each histogram.

Tab. S1. Summary of all dynamic SMFS data of HA_4HB_4, measured in the absence and the presence of 1 mM $NiCl_2$. Data shown in Fig. S3 and S4 are marked in bold. *Data measured at a retract speed of 4000 nm s^{-1}.

cantilever		**1**			**2**			**3**		
sample	speed [nm s^{-1}]	F_R [pN]	$\dot{F}$ [pN s^{-1}]	*n*	F_R [pN]	$\dot{F}$ [pN s^{-1}]	*n*	F_R [pN]	$\dot{F}$ [pN s^{-1}]	*n*
HA_4HB_4	50	**27.8**	**30**	**334**	28.7	49	145	24.7	32	164
	200	**32.3**	**129**	**207**	31	202	95	28.1	134	92
	400	**33.8**	**298**	**251**	31.7	461	230	32.3	317	170
	1000	**37.9**	**924**	**272**	36.2	1606	63	34.1	926	254
	2500	**42.5**	**3231**	**126**	40.8	5006	54	42.8	3047	72
	5000	**50.7**	**10051**	**88**	49.4	11715	33	-	-	-
HA_4HB_4 + Ni^{2+}	50	34.4	32	341	32.9	34.4	132	**36.8**	**33.8**	**204**
	200	38.5	159	172	43.6	190	150	**39.7**	**133**	**55**
	400	41.4	351	227	44.4	431	131	**43.6**	**295**	**124**
	1000	43.4	1084	232	50.7	1281	122	**47.2**	**953**	**126**
	2500	54.6	4037	76	53.1	4134	154	**49**	**2691**	**99**
	5000	56.4*	4513*	28	-	-	-	**56.2**	**6488**	**60**

For each of the three cantilevers, the values of the most probable rupture force were plotted against the logarithm of the corresponding loading rate. The data was fitted with the Bell-Evans model[10] (**Equation 3**) to determine the extrapolated thermal off-rate at zero force (k_{off}) and the potential width Δx at a given temperature *T* (25 °C):

$$F_R(\dot{F}) = \frac{k_B T}{\Delta x} \cdot \ln \frac{\dot{F} \cdot \Delta x}{k_B T \cdot k_{off}} \quad (Equation\ 3)$$

The obtained fit values, k_{off} and Δx, as well as their mean ± SEM are summarized in **Tab. S2**. In the presence of Ni^{2+}, HA_4HB_4 is almost one order of magnitude more stable (lower k_{off}) than in the absence of Ni^{2+}. In contrast, Δx is not affected significantly by the presence of Ni^{2+}.

Tab. S2. Results of the Bell-Evans fit for HA_4HB_4, measured in the absence and the presence of Ni^{2+}.

Sample	**HA_4HB_4**		**HA_4HB_4 + Ni^{2+}**	
Parameter	k_{off} [s^{-1}]	Δx [nm]	k_{off} [s^{-1}]	Δx [nm]
1	$6.9 \cdot 10^{-3}$	1.10	$4.8 \cdot 10^{-3}$	0.94
2	$8.7 \cdot 10^{-3}$	1.16	$2.4 \cdot 10^{-3}$	0.98
3	$17.5 \cdot 10^{-3}$	1.08	$0.3 \cdot 10^{-3}$	1.18
Mean ± SEM	**$11.0 \pm 3.3 \cdot 10^{-3}$**	**1.11 ± 0.02**	**$2.5 \pm 1.3 \cdot 10^{-3}$**	**1.03 ± 0.07**

4 Hydrogel preparation and oscillatory shear rheology

The cysteine-containing peptides were used to synthesize HA_4HB_4 crosslinked PEG hydrogels, based on maleimide-functionalized star-shaped polyethyleneglycol (sPEG). For hydrogel synthesis, the individual peptides were first dissolved in PBS (10 mM Na_2HPO_4, 2 mM KH_2PO_4 137 mM NaCl, 2.7 mM KCl, pH 7.4) in a concentration of 10 mg ml^{-1}. To ensure that all peptides are available for reaction with sPEG-maleimide, possible disulfide bonds were reduced with Pierce™ Immobilized TCEP Disulfide Reducing Gel (Thermofisher Scientific) for 1.5 h at 4 °C on a mixer (2000 rpm). The reduced peptides were coupled to sPEG (40 kDa, 4-arm; Jenkem Technology) separately to obtain sPEG-HA_4 and sPEG-HB_4. A 1.2-fold to 1.5-fold excess of peptide was used to ensure that all arms of sPEG are functionalized. After incubating the reaction mixture for 30 min (RT, 800 rpm), the excess of peptide was removed using ultrafiltration (molecular weight cut-off 10 kDa). During ultrafiltration (5x, 14000 g for 10 min) the buffer was exchanged to ultrapure water. The purified sPEG-peptide conjugates were lyophilized and redissolved in PIPPS BS (pH 8.1) to a concentration of 0.5 mM. sPEG-HA_4 and sPEG-HB_4 were mixed in a ratio of 1:1 to induce CC formation. Hydrogels formed in less than 1 min. Air bubbles entrapped in the hydrogel were removed by centrifugation for 2 min at 2000 g. To study the effect of Ni^{2+} coordination, $NiCl_2$ was added in a ratio of 1:1 His:Ni^{2+}. The reversibility of metal ion coordination was investigated by adding EDTA to a final concentration of 10 mM.

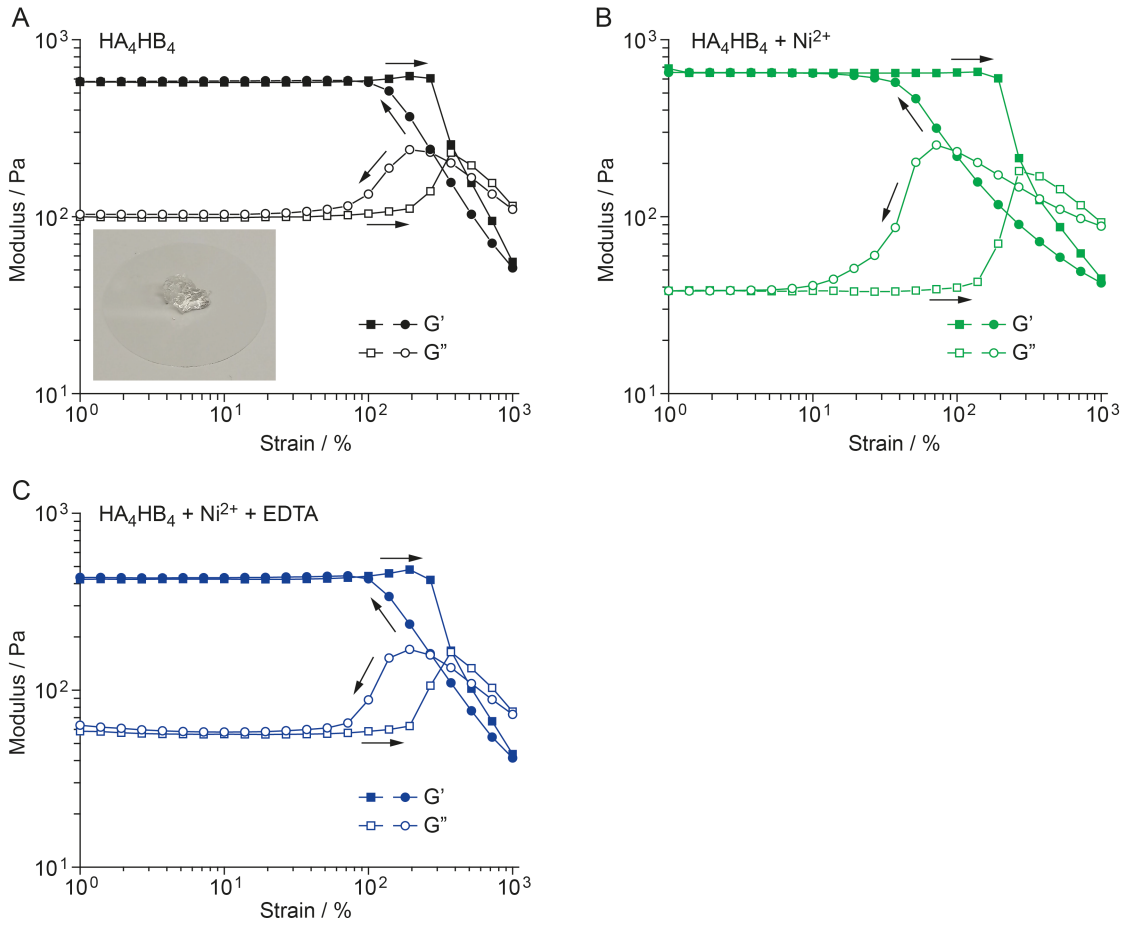

Fig. S6. Amplitude sweeps of the CC crosslinked hydrogels (angular frequency of 10 rad s^{-1}). A) Measurement performed in the absence of Ni^{2+}. Inset: picture of the hydrogel. B) Measurement performed in the presence of Ni^{2+} (4 mM $NiCl_2$). C) Measurement performed in the presence of 4 mM $NiCl_2$ and 10 mM EDTA. The amplitude sweeps were conducted from 1 % to 1000 % stain and back from 1000 % to 1 % to test for self-healing.

The resulting hydrogels were characterized with strain-controlled oscillatory shear rheology (MCR 301, Anton Paar), using a 12 mm diameter cone-plate geometry (CP12-1, angle 1°, Anton Paar). The gap width was adjusted to 0.02 mm. The rheometer was equipped with a temperature controlled hood (25 °C) to prevent evaporation. To determine the linear viscoelastic range, amplitude sweeps were performed ranging from 1 % to 1000 % shear strain (**Fig. S6**) and vice versa. During the amplitude sweeps, the frequency was kept constant at 10 rad s^{-1}. After a short resting time of 2 min, a frequency sweep was conducted from 0.001 or 0.002 rad s^{-1} to 100 rad s^{-1}. During the frequency sweeps, the strain amplitude was kept constant at a strain of 1 %, which lies in the linear viscoelastic range. Frequency sweeps were used to obtain information about the dynamic viscoelastic properties (**Fig. 4** in the main text). The relaxation time τ of the non-covalent crosslinks can be obtained from the crossover point of *G'* and *G"* in the frequency sweep. **Tab. S3** contains an overview of the

relaxation times obtained from three independent measurements at each different condition.

Tab. S3. Relaxation time τ of the CC-crosslinked sPEG hydrogels. Shown are the values obtained from three independent measurements, including the mean ± SEM.

Sample	**no metal**	**1:1 His:Ni^{2+}**	**Ni^{2+} + EDTA**
Parameter	τ [s]	τ [s]	τ [s]
1	72	270	50
2	135	286	33
3	70	217	48
Mean ± SEM	**92 ± 12**	**258 ± 36**	**44 ± 4**

5 References

1. S. M. Kelly, T. J. Jess and N. C. Price, *Biochim. Biophys. Acta*, 2005, **1751**, 119.
2. S. Y. Lau, A. K. Taneja and R. S. Hodges, *J. Biol. Chem.*, 1984, **259**, 13253.
3. C. Aronsson, S. Dånmark, F. Zhou, P. Öberg, K. Enander, H. Su and D. Aili, *Sci. Rep.*, 2015, **5**, 14063.
4. J. L. Zimmermann, T. Nicolaus, G. Neuert and K. Blank, *Nat. Protoc.*, 2010, **5**, 975.
5. J. L. Hutter and J. Bechhoefer, *Rev. Sci. Instrum.* , 1993, **64**, 1868.
6. F. Oesterhelt, Rief, M., Gaub, H.E., *New J. Phys.*, 1999, **1**, 6.1.
7. J. N. Milstein and J.-C. Meiners, in *Encyclopedia of Biophysics*, ed. G. C. K. Roberts, Springer Berlin Heidelberg, Berlin, Heidelberg, 2013, pp. 2757.
8. F. Kienberger, V. P. Pastushenko, G. Kada, H. J. Gruber, C. Riener, H. Schindler and P. Hinterdorfer, *Single Mol.*, 2000, **1**, 123.
9. T. Hugel and M. Seitz, *Macromol. Rapid Commun.*, 2001, **22**, 989.
10. E. Evans, *Annu. Rev. Biophys. Biomol. Struct.*, 2001, **30**, 105.

6 Author contributions

I.T., A.S.L, K.G.B. and M.J.H. designed the experiments. I.T. carried out and analyzed the experiments. A.S.L. set up the rheology experiments and contributed to analyzing and interpreting the hydrogels results. I.T., A.S.L., K.G.B and M.J.H. discussed the results. I.T., K.G.B. and M.J.H. wrote the manuscript.